GC PS-Wave Azimuthal Anisotropy: Benefits for Fractured Reservoir*

By
James E. Gaiser[1]
Search and Discovery Article #40120 (2004)

*Adapted from the Geophysical Corner columns in AAPG Explorer, April and May, 2003, entitled, respectively, "Reservoir Cracks Tell Many Tales" and "Stress Direction Hints at Flow," and prepared by the author. Appreciation is expressed to the author, to R. Randy Ray, Chairman of the AAPG Geophysical Integration Committee, and to Larry Nation, AAPG Communications Director, for their support of this online version.

[1]Geophysical Advisor, WesternGeco, Denver, Colorado (jgaiser@denver.westerngeco.slb.com)

Introduction

There are many known fractured reservoirs worldwide that have been profitably produced, but it is safe to say that none of them have been depleted efficiently. As production costs rise and our industry focuses more on production and development, it is becoming crucial to recognize the influence of fractures early in the life of a field for optimal reservoir management. An important part of this management begins with the classification of fractured reservoirs based on production issues, such as rates and reserves.

Fractures have a significant effect on permeability, resulting in preferred directions of flow, and they are probably more common than we think. A key strategy for fractured reservoir management is an accurate description of the geological, geophysical, and petrophysical attributes of fractures within the reservoir. Traditionally this information comes from well data and, to some extent, large-scale seismic features (observable faults).

This article describes how sub-seismic attributes of azimuthal anisotropy can potentially add to this characterization of a fractured reservoir.

PS-Waves

Converted waves (PS-waves), created by traditional downgoing compressional waves (P-waves) that reflect as shear-waves (S-waves), provide us with a unique ability to measure anisotropic seismic attributes that are sensitive to fractures. Solutions that PS-wave anisotropy can bring to fractured reservoir management are:

- Sweet-spot detection.
- Improved models for reservoir simulation.
- Production history matching.
- Time-lapse behavior of fracture properties over the life of a field (most important for dynamic management).

The goal, of course, is to reduce the total production costs for reservoir depletion by using fracture information as early as possible.

Fractured Reservoir Types

It is well known that porosity and permeability are key factors used to describe fractured reservoirs. As a motivation for the need of azimuthal anisotropy measurements, Figure 1 shows a schematic distribution of different reservoir types in terms of percent total porosity and total permeability (Nelson, 2001).

A Type I fractured reservoir is where fractures dominate both porosity and permeability. Most of the reserves are stored in the fractures, and flow is confined within them. These are very heterogeneous and anisotropic reservoirs.

At the other end of this distribution are Type IV reservoirs, where fractures provide no additional permeability or porosity. Ideally this would be a homogeneous "tank" reservoir when no fractures are present -- but when they are present, fractures can sometimes be a problem and act as barriers to flow.

Type II and Type III fractured reservoirs are of an intermediate nature where fractures control permeability and assist permeability, respectively. In these two cases, more reserves are stored within the matrix, but fractures still have an impact and can result in anisotropic permeability and unusual response to secondary recovery (elliptical drainage).

Bottom line: In going from Type IV to Type I, there is an increasing effect of fractures.

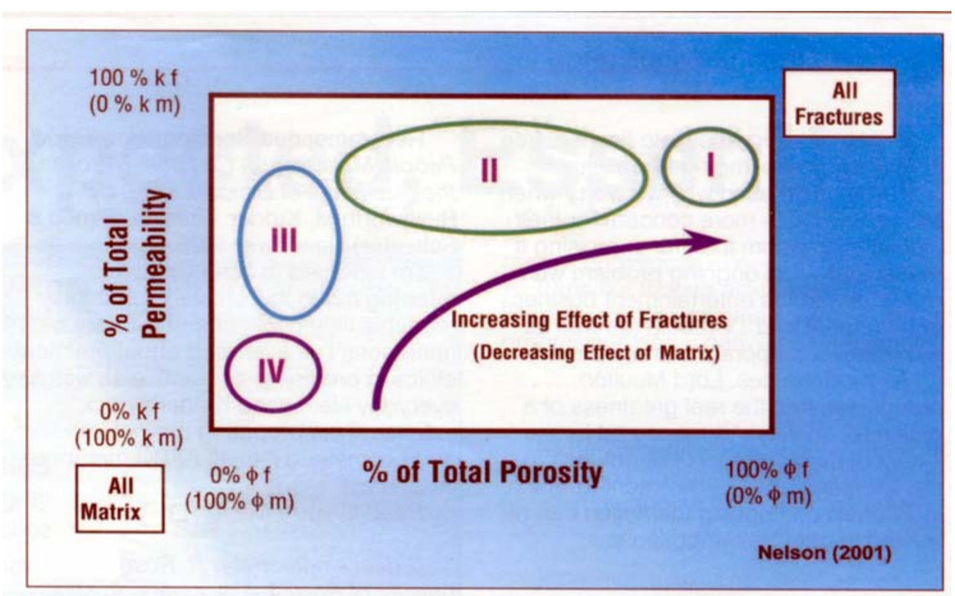

Figure 1. Schematic distribution of fractured reservoir types. Type I is fracture-dominated; Type IV is matrix-dominated; Types II and III are where fractures control permeability and assist permeability, respectively.

Fractures and PS-Wave Seismic Data

Fracture properties are fractal by nature, as illustrated in Figure 2. Cores and image logs typically provide the small-scale features of the reservoir and surface-seismic data can provide the largest scale features like faults with large displacements. Each tool yields a portion of the total fracture network; however, it is clear that these end members alone do not control production. If they did, reservoir models and fluid simulations would be perfect.

Fracture properties over the intermediate range of scales in Figure 2 are missing. Traditionally this has been filled with paleo-strain fields that relate to possible fracture directions and intensities, inferred from geomechanical modeling by palinspastic reconstruction. This method, however, can be highly non-unique and uncertain in the presence of unconformities.

Azimuthal anisotropy measurements can be used for this sub-seismic resolution. Although fractures are smaller than a seismic wavelength and individual fractures are not directly observed, we do get an average response. This averaging leads to a directional dependence; i.e., our velocities are azimuthally anisotropic.

We can measure anisotropy at the borehole with vertical seismic profiles (VSPs) and with P-wave surface seismic data, but I want to focus on the use of PS-waves. Figure 3 illustrates a typical PS-wave source-receiver geometry. The most important property is the azimuth or the propagation direction from source to receive. We need to sample a full range of azimuths over 360 degrees for azimuthal anisotropy measurements.

In addition to the P-waves that reflect at a common midpoint (CMP), we detect PS-waves that convert at common-conversion points (CCP), using three-component (3C) geophones. The source-to-detector azimuth controls the direction of polarization of the created S-wave, but this upgoing S-wave immediately splits and travels to the surface as two orthogonally polarized S-waves.

Figure 4 shows a more detailed view of S-wave splitting for a single set of vertical fractures, simulated by a grid that is oriented north-south. The upgoing converted S-wave travels as a fast and slow component that is polarized parallel and perpendicular to the fractures, respectively. The time difference between them depends on the percent S-wave anisotropy and is proportional to fracture density.

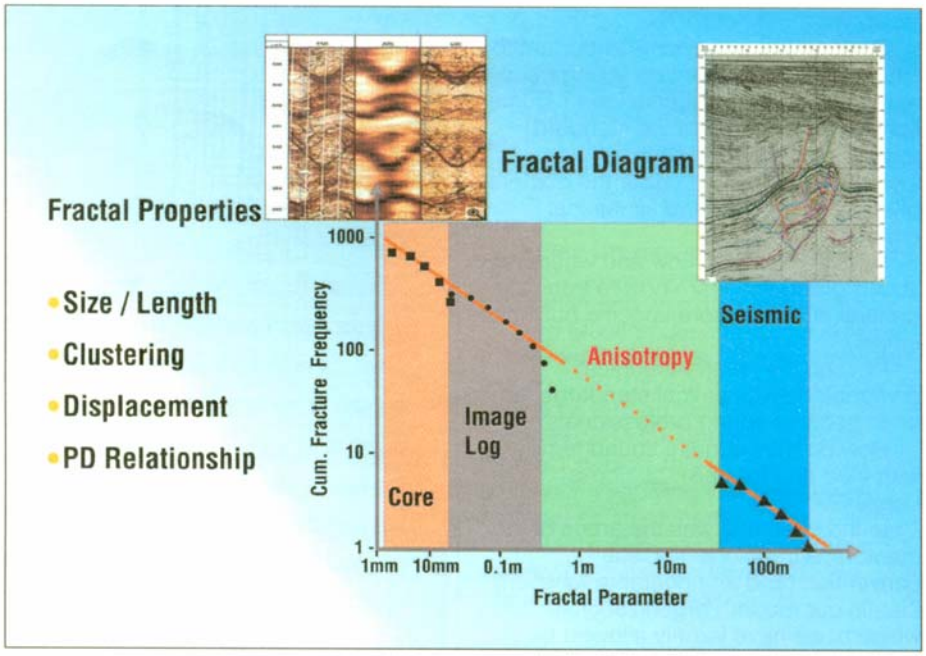

Figure 2. Quantitative studies of fractures show they are fractal by nature (from Mattner, 2002). Measurements of seismic anisotropy best characterize fracture scales in the mid-range between 1 meter and 100 meters.

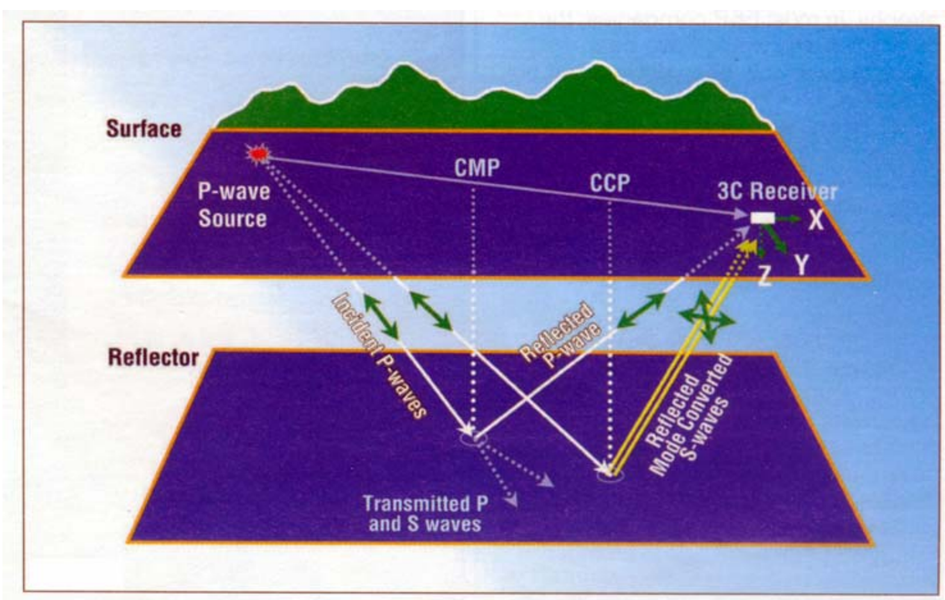

Figure 3. Converted-wave survey geometry where the P-wave common mid-point (CMP) is in a different location than the converted PS-wave common-converted midpoint (CCP). To measure azimuthal anisotropy reliably, it is important to sample a full range of source-receiver azimuths over 360 degrees.

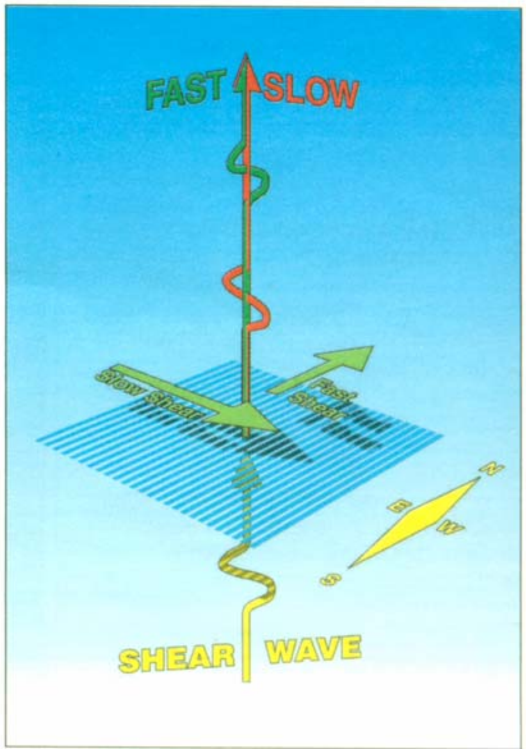

Figure 4. Shear-wave splitting in an anisotropic medium, where the fast-shear wave is polarized parallel to fractures and is orthogonal to the slow-shear wave.

PS-Wave Data Example: North Sea Subsidence Stress

The algorithm used for fracture characterization is a layer-stripping method that consists of first finding an optimal rotation of the horizontal components to separate fast and slow S-waves by Alford rotation. This provides the fast S-wave direction (fracture orientation). Then correlation of the fast and slow S-wave provides time delays for estimates of the amount of splitting and fracture density information.

Figure 5 shows the results from the shallow overburden at the Valhall Field in the North Sea. A 3-D ocean bottom cable (OBC) survey was acquired there in 1998 using wide-azimuth source-receiver geometry to provide a full range of azimuth data.

The small vectors show the orientation of the fast shear-wave direction, oriented NNW by SSE, as measured along the receiver lines, and the length of these vectors is proportional to the time lag or percent anisotropy (maximum is about 3 percent). A simple interpretation of this display is that the vectors represent a single set of vertical fractures seen from above.

Note the interesting concentric pattern centered on the production platform (red triangle). This is a dramatic example where man-made alterations of the subsurface have induced horizontal-stress perturbations near the surface.

The pattern of S-wave splitting correlates precisely with subsidence at the platform due to collapse of the reservoir. In the center where there has been four meters of subsidence the anisotropy is relatively small, but as one moves away from the center, there is an increase in the anisotropy along the flanks of the subsidence where radial extension is occurring. Here is where the minimum horizontal stress direction is radial, and the maximum horizontal stress direction is transverse. This agrees exactly with the fast S-wave orientation, and it is a good example showing that the fast S-wave direction is highly sensitive to the maximum horizontal stress direction.

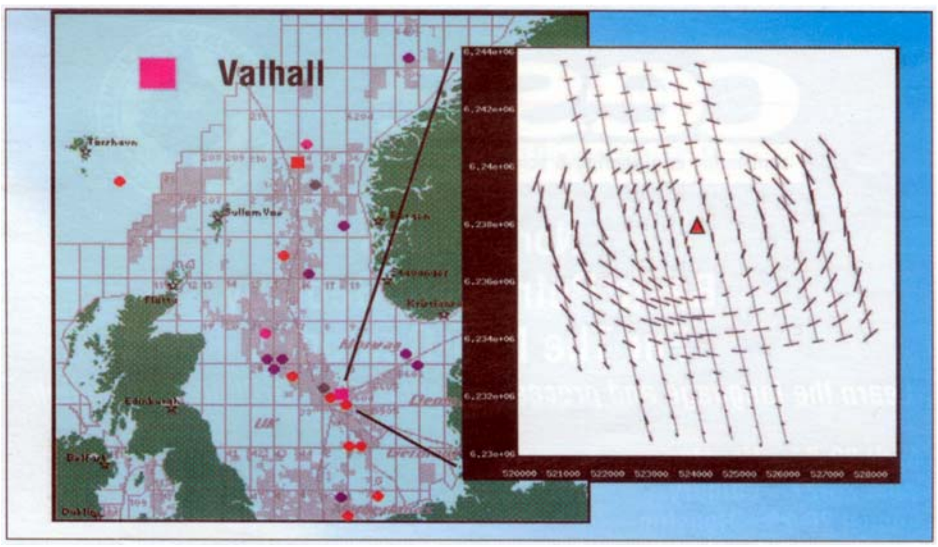

Figure 5. Valhall Field in the North Sea shows a concentric pattern of fast shear waves that correspond to subsidence around the producing platform (red triangle). This is a good example showing that the fast shear-wave direction is highly sensitive to the maximum horizontal stress direction.

Advanced Applications

Unfortunately the situation is a bit more complicated than that described in the Valhall example, and advanced applications of seismic azimuthal anisotropy are required. Figure 6 shows that the complexity of S-wave splitting can increase with the distance of travel. The separate fast and slow waves produced by the initial PS-wave in the first (lower) anisotropic layer encountered can split again within the next (upper) anisotropic layer above.

In addition, each rock layer can have a different orientation of fractures (coordinate frame) and different fracture density. The various split S-wave modes are combined when detected by the two horizontal geophones. In order to estimate the azimuthal anisotropy (fracture properties) at the target, we need to unravel the data by layer-stripping in a top-down fashion. As a result, the overburden anisotropy must be determined and removed first. The results at Valhall Field (Figure 5) represent an estimate of this overburden anisotropy.

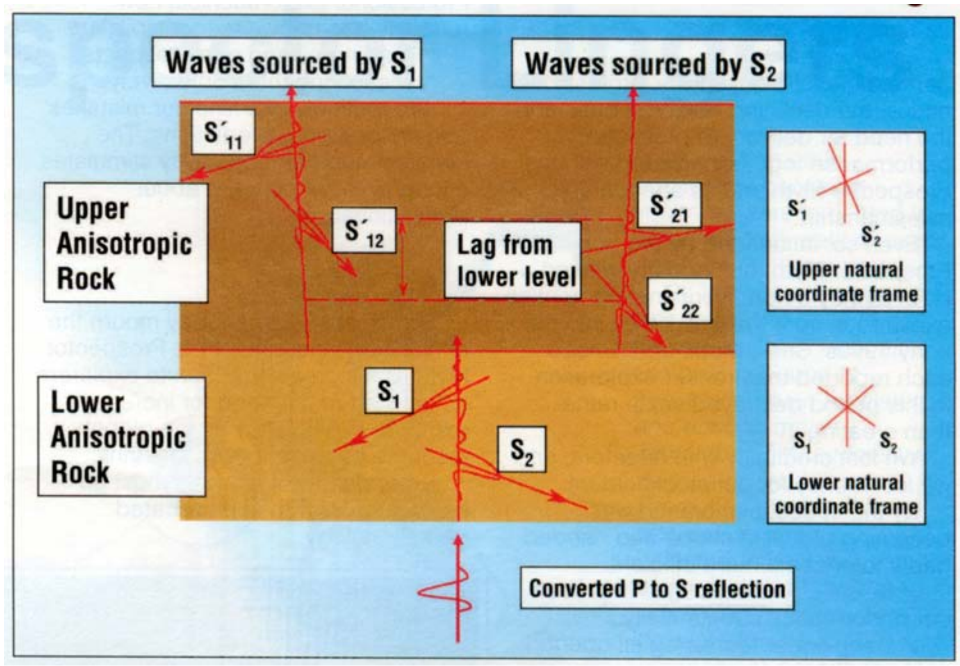

Figure 6. Diagram of upgoing PS-waves, showing that the separate fast and slow waves produced by the initial PS-wave in the first (lower) anisotropic layer encountered can split again within the next (upper) anisotropic layer above. The various split S-wave modes are combined when detected by the two horizontal geophones and must be unraveled by layer-stripping to estimate the azimuthal anisotropy (fracture properties).

PS-wave Data Example: Wyoming Fractured Gas Sands

Several land examples from Wyoming were acquired to investigate naturally fractured gas sands. Two of these, from the Green River Basin, show similarities in the orientation of the fast S-wave and amount of anisotropy in the overburden, as well as fracture-related anisotropy associated with faults and lineaments.

Another example is the Madden Field from the Wind River Basin (Figure 7). Naturally fractured tight gas sands in the Tertiary Lower Fort Union formation produce from depths of 4500 to 9000 feet. A 3-D seismic survey covering 15 square miles over the crest of the field shows the fault trends (bold east-west lines). The seismic data were acquired using dynamite with 20 pound charges set at a depth of 60 feet.

The important attributes are shown in Figure 7, the percent anisotropy in color, from zero to 9 percent over the Lower Fort Union (at 2.2 to 3.3 seconds reflection time) after correcting for overburden anisotropy by layer-stripping, and the fast S-wave orientation by small vectors whose length is proportional to percent anisotropy.

The interesting point here is that variations in percent anisotropy appear to be controlled by the faults; the orientation of the fast S-wave is usually oblique to them. Areas of high percentage of anisotropy may represent sweet spots of concentrated fracturing or fracture swarms.

Although fracture properties have not been directly calibrated with anisotropy measurements from borehole data in the survey area, a VSP outside the area showed changes in anisotropy (S-wave orientation) between the overburden and Lower Fort Union that are similar to the PS-wave anisotropy.

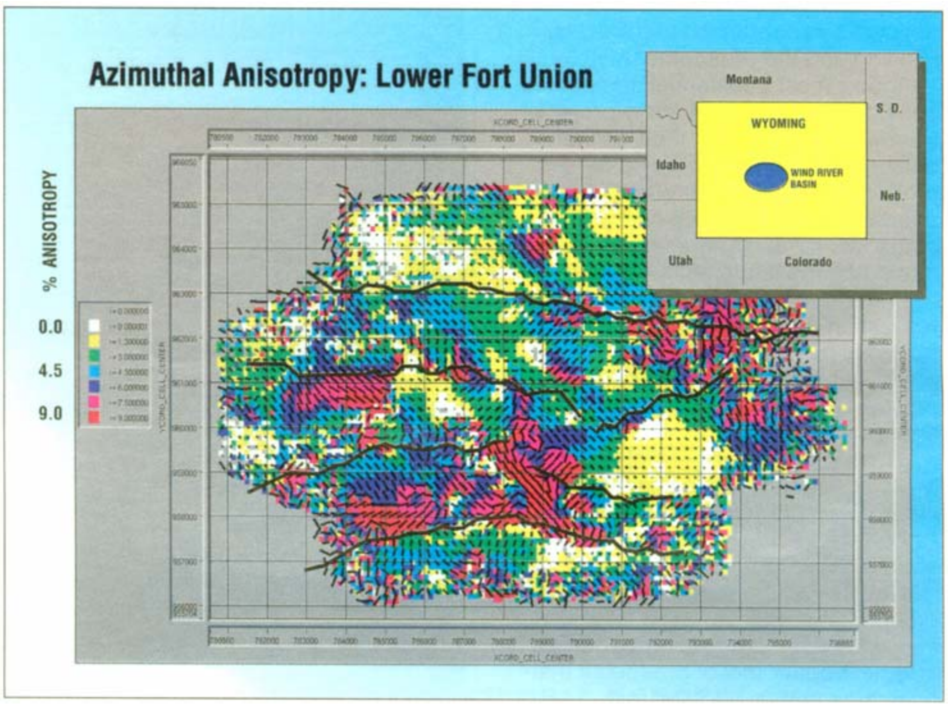

Figure 7. Madden Field in the Wind River Basin, Wyoming, shows percent anisotropy in color from zero to 9 percent over the Lower Fort Union (2.2 to 3.3 seconds) and the fast S-wave orientation by small vectors. Areas of high percentage of anisotropy may represent sweet spots of concentrated fracturing or fracture swarms.

PS-wave Data Example: Adriatic Fractured Carbonate

The next example (Figure 8) is from the Adriatic Sea, offshore Italy, where the target is the naturally fractured upper Paleocene Scaglia carbonate. Significant east-west tectonic compression creates north-south anticlinal structures where commercial quantities of gas have accumulated in fractured zones.

The operators (Agip) acquired an ocean bottom cable (OBC) seismic survey to help them position two horizontal wells for optimal recovery. The fast S-wave direction shown in color illustrates the bimodal distribution associated with the target layer. Yellows and oranges are oriented roughly east-west, and blues and greens north-south.

Note the compartmentalization and apparent control by faulting (thin black lines). Where faults and anticlinal structure (thick red arrows) change direction in the south, there is also a change in the fast S-wave direction (browns and dark blues).

The most important result is the good agreement with the borehole data in wells at the top of the structure (white points). From breakout analysis and induced fracture studies, the maximum horizontal stress is consistently about N70E. This agrees with P-wave fast directions determined from AVO analyses as a function of azimuth.

Based on production, borehole fracture studies and anisotropy from seismic data, the Emilio Field has characteristics of a Type II fractured reservoir. Out of the small number of wells drilled, only a few are highly productive. Although there may be some secondary matrix or vuggy porosity, it appears that fractures control the permeability and have a significant impact on the production.

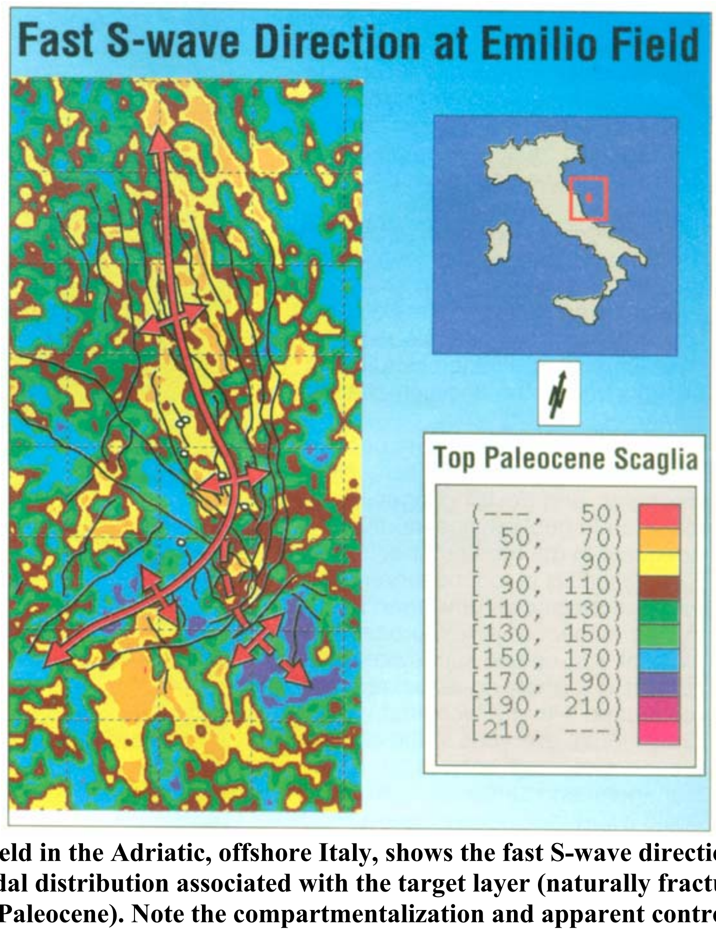

Figure 8. Emilio Field in the Adriatic, offshore Italy, shows the fast S-wave direction in color to illustrate the bimodal distribution associated with the target layer (naturally fractured Scaglia carbonates, upper Paleocene). Note the compartmentalization and apparent control by faulting (thin black lines). There is good agreement with the borehole data in wells at the top of the structure (white points), and based on production, borehole fracture studies and anisotropy from seismic data, the Emilio Field has characteristics of a Type II fractured reservoir.

Fracture Characterization Technology

Historically the classification of Type I (fracture-dominated) to Type IV (matrix-dominated) reservoirs has proved to be quite useful. Figure 9 is a graph, also from Nelson (2001), showing examples from several reservoirs where the percentage of wells are ordered from the least to the most productive, nd the vertical axis is cumulative production. The different fractured reservoirs correlate nicely with these production characteristics.

For the Type I, fracture-dominated heterogeneous reservoirs, a small percentage of wells contribute to most of the production, and there are many dry and marginal wells. As we transition through the other types, the curves become straighter, and more wells contribute equally to the total production. The 45-degree line corresponds to a homogeneous-isotropic, matrix-dominated reservoir where all wells contribute equally.

Nelson has quantified these fractured reservoir types by a "Fracture Impact Coefficient." He points out that this is not necessarily a physical property of the reservoir, but is instead a result of drilling fields on regular grids without exploiting the presence of fractures -- something he calls "fracture denial." Consequently, it might be more appropriate to call this quantity the "Fracture Denial Coefficient," because it appears to be directly proportional with fractured reservoir type and ranges between 0.28 -- 0.73.

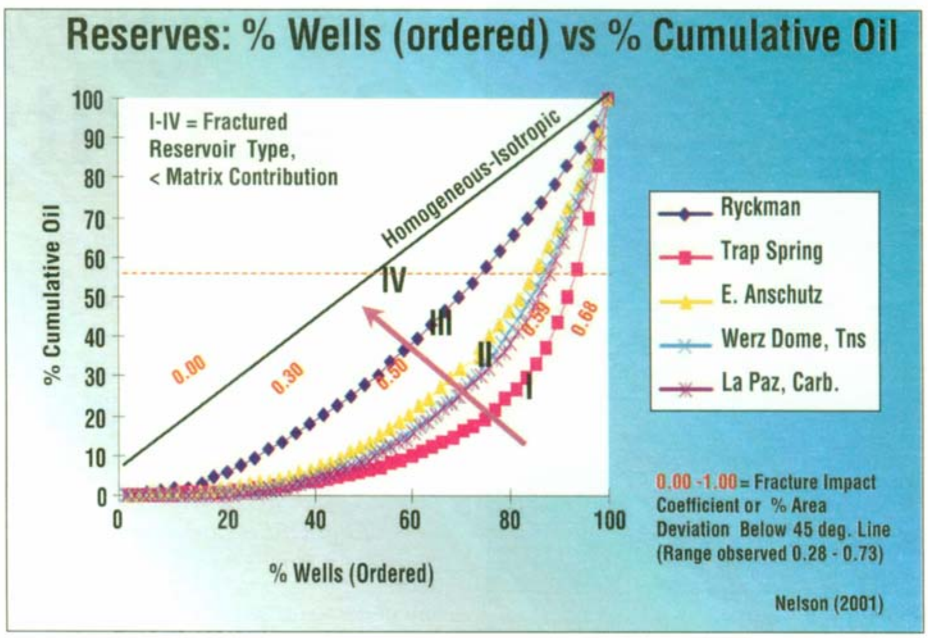

Figure 9. Graph that shows examples from several reservoirs where percentage of wells are ordered from the least to the most productive and the vertical axis is cumulative production. The different fractured reservoir types correlate nicely with these production characteristics and the "fracture impact coefficient." Our goal is to avoid the scenario of unproductive wells in the lower left corner of the graph by characterizing fractures as early as possible.

Ultimately our goal is to avoid the scenario of unproductive wells in the lower left corner of the graph in Figure 9 by using every tool at our disposal to characterize fractures as early as possible for efficient reservoir depletion. One of these tools can be PS-wave data for measuring azimuthal anisotropy and the heterogeneity related to fractures.

Conclusion

The examples presented in these articles suggest that azimuthal anisotropy can be measured with wide-azimuth PS-wave surveys and that S-wave splitting is highly sensitive to the maximum horizontal stress direction. Knowing these maximum stress directions, which are aligned with open fractures when the differential stress is large enough, provides valuable information about preferred reservoir flow directions.

Potentially, PS-wave data could become an integral part of fracture sweet-spot detection, reservoir model building/simulation,and dynamic reservoir management through the use of time-lapse surveys. However, to utilize this technology optimally, it is important to calibrate results with ground truth for incorporating into reservoir models. One approach is VSP data to acquire azimuthal S-wave information at the same scale as surface-seismic data. Dipole sonic and FMI logs are also valuable for characterizing small-scale fracture properties that can be related to larger scale features.

It also is important to improve our resolution with smaller seismic time windows and more accurate anisotropy models that include dipping fracture properties. However, these will have to be the subject of future research.

Acknowledgments

The author thanks Rich Van Dok, Richard Walters and Bjorn Olofsson from WesternGeco, for their expertise in data processing of the Madden, Emilio, and Valhall studies, respectively; and also Lynn Inc., Eni/Agip division, BP, and WesternGeco for their support and permission to publish this material.

References

Nelson, R.A., 2001, Geologic analysis of naturally occurring fractured reservoirs (2nd edition): Gulf Professional Publishing, Boston, 332 p.

Mattner, Joerg, 2002, Fractured reservoir characterization from collecting data to dynamic modeling: Course, GeoTech Consulting, slide (as part of presentation).